PNAS RESEARCH ARTICLE | MICROBIOLOGY

A proteolytic pathway coordinates cell division and heterocyst differentiation in the cyanobacterium *Anabaena* sp. PCC 7120

Wei-Yue Xing[a], Jing Liu[a,b], Ju-Yuan Zhang[a], Xiaoli Zeng[a], and Cheng-Cai Zhang[a,c,d,1]

Edited by Susan Golden, University of California San Diego, La Jolla, CA; received May 10, 2022; accepted August 2, 2022

The filamentous, multicellular cyanobacterium *Anabaena* sp. PCC 7120 (*Anabaena*) is a prokaryotic model for the study of cell differentiation and cell-cell interactions. Upon combined-nitrogen deprivation, *Anabaena* forms a particular cell type, heterocyst, for aerobic nitrogen fixation. Heterocysts are semiregularly spaced among vegetative cells. Heterocyst differentiation is coupled to cell division, but the underlying mechanism remains unclear. This mechanism could be mediated by the putative protease HetF, which is a divisome component and is necessary for heterocyst differentiation. In this study, by suppressor screening, we identified PatU3, as a negative regulator acting downstream of HetF for cell division and heterocyst development. The inactivation of *patU3* restored the capacity of cell division and heterocyst differentiation in the Δ*hetF* mutant, and overexpression of *patU3* inhibited both processes in the wild-type background. We demonstrated that PatU3 was a specific substrate of the protease activity of HetF. Consequently, PatU3 accumulated in the *hetF*-deficient mutant, which was responsible for the resultant mutant phenotype. The cleavage site of PatU3 by HetF was mapped after the Arg117 residue, whose mutation made PatU3 resistant to HetF processing, and mimicked the effect of *hetF* deletion. Our results provided evidence that HetF regulated cell division and heterocyst differentiation by controlling the inhibitory effects of PatU3. This proteolytic pathway constituted a mechanism for the coordination between cell division and differentiation in a prokaryotic model used for studies on developmental biology and multicellularity.

protease | divisome | cyanobacteria | cell-division inhibitor | peptidoglycan

Significance

Protein degradation is an important regulation mechanism in biology. Although HetF has long been predicted to be a putative protease in the filamentous cyanobacterium *Anabaena* sp. PCC 7120, its activity or substrate has never been demonstrated. In this study, we provided *in vitro* and *in vivo* evidence for the protease activity of HetF acting on PatU3 as a specific substrate. The degradation of PatU3 by HetF relieves the inhibitory effects of PatU3 on cell division and heterocyst development, thus providing a mechanism for the coordination of the two biological processes. The proteolytic system reported here enriched our understanding on the control mechanism for cell division and development in cyanobacteria.

In developmental organisms, cell cycle is modulated so that a cell can be engaged into a developmental process. In eukaryotes, cell cycle regulators play key roles in developmental processes (1). The cyanobacterium *Anabaena* (*Nostoc*) sp. PCC 7120 (hereafter *Anabaena*) is a multicellular and filamentous prokaryote, and a model used for studying bacterial cell development. In *Anabaena* filaments, 5 to 10% of the vegetative cells differentiate into heterocysts in response to combined nitrogen step-down or carbon oversupply, whereas heterocyst differentiation is repressed in the presence of a combined nitrogen source such as nitrate or ammonium (2–4). Heterocysts are semiregularly intercalated among vegetative cells. They provide fixed nitrogen to neighboring vegetative cells and receive in return photosynthetic carbohydrates (2–4). Heterocyst differentiation lasts 20 to 24 h, and the transcription factor HetR is a master regulator necessary and sufficient for this process (5, 6). When *hetR* is inactivated, no heterocyst differentiation occurs, whereas overexpression of *hetR* results in multiple contiguous heterocysts (Mch) even under repressive conditions (5, 6). HetR activates the expression of *hetZ* and *hetP*, which act together so that the differentiation reaches the commitment step, defined as the point of no return in the process of heterocyst differentiation (2, 7–11). Overexpression of *hetZ* and *hetP* together can partially bypass HetR for heterocyst differentiation (10, 11). After the commitment step, the developing cells become terminally differentiated, unable to reverse back to vegetative stage. At the end of the developmental process, morphogenesis takes place with the thickening of the existing peptidoglycan (PG) layer and the formation of two additional layers of the cell wall, a glycolipid layer and a polysaccharide layer (2, 12). The morphological modifications, combined with metabolic reprogramming, create a microoxic environment in heterocysts suitable for N_2 fixation (2, 4).

Heterocyst pattern is established and maintained along the filaments by possible morphogen gradients of both positive regulators such as HetR, and negative regulators such as PatS, PatX, and HetN (2, 5, 6, 13–18). Another regulator, PatU3, has also been identified for its role in heterocyst pattern formation (19). Inactivation of *patU3* led to the Mch phenotype, as well as cells smaller in size, indicating that PatU3 acted as an inhibitor of heterocyst formation, and maybe, of cell division (19). It was proposed that PatU3 regulated cell size through the interaction with Ftn6 (20), a divisome component specific to cyanobacteria (21–23). *patU3* is located in an operon together

Author affiliations: [a]State Key Laboratory of Freshwater Ecology and Biotechnology, Key Laboratory of Algal Biology, Institute of Hydrobiology, Chinese Academy of Sciences, Wuhan, Hubei 430070, China; [b]University of Chinese Academy of Sciences, Beijing 100049, China; [c]Institut WUT-AMU, Aix-Marseille Université and Wuhan University of Technology, Wuhan, Hubei 430070, China; and [d]Innovation Academy for Seed Design, Chinese Academy of Sciences, Beijing 100049, China

Author contributions: C.-C.Z. designed research; W.-Y.X. and J.L. performed research; W.-Y.X., J.-Y.Z., and X.Z. analyzed data; and W.-Y.X., J.-Y.Z., and C.-C.Z. wrote the paper.

The authors declare no competing interest.

This article is a PNAS Direct Submission.

[1]To whom correspondence may be addressed. Email: cczhang@ihb.ac.cn.

This article contains supporting information online at http://www.pnas.org/lookup/suppl/doi:10.1073/pnas.2207963119/-/DCSupplemental.

Published August 29, 2022.

with *hetZ* (19). Inactivation of *hetZ* prevents heterocyst differentiation, while overexpression of *hetZ* leads to Mch (19, 24). HetZ is shown to interact with PatU3 (25), which may constitute a mechanism for the inhibitory effect of PatU3 on heterocyst formation.

Cell division is intimately linked to heterocyst development in *Anabaena*. Indeed, once cell division is blocked by the inactivation or inhibition of certain components of the divisome, heterocyst development is suppressed (26, 27). The early step of bacterial cell division is initiated by FtsZ, a tubulin-like cytoskeleton forming a ring-like structure at the midcell position (28). FtsZ recruits other proteins to form a large complex, called divisome, for cell division (29). At the late step of cell division, PG remodeling, catalyzed by enzymes of the divisome, occurs for cell constriction and septation. In *Anabaena*, FtsZ plays a role not only in cell division, but also in heterocyst development (30). The HetF protein appears to be a critical link between cell division and heterocyst differentiation (27). HetF was proposed to play a role at the early steps of heterocyst development (31–33), but its relationship with other heterocyst regulators is poorly defined. It has been shown that ectopic expression of *hetZ* could suppress the phenotype of *hetF* in heterocyst differentiation, suggesting that *hetF* could control the commitment step through *hetZ* (11). HetF participates directly in cell division as a member of the divisome in *Anabaena*, and its function in cell division is enhanced when cells are under high-light illumination (27). HetF interacts with FtsI (PBP3), and the latter is an enzyme for septal PG synthesis. Accordingly, in the absence of *hetF*, FtsZ was still able to assemble into ring-like structures at the midcell position for the initiation of cell division, but septal PG synthesis was abolished (27). It is still unknown how HetF coordinates cell division and heterocyst development. It is also puzzling that in the absence of *hetF*, HetR level is dramatically increased in all cells along the filaments of *Anabaena* without causing Mch, not even the formation of spaced single heterocysts (32), whereas increasing *hetR* expression in the wild-type (WT) background is known to stimulate heterocyst differentiation, including the formation of Mch (6).

In this study, we report the identification of PatU3 as a cell-division inhibitor and a specific substrate of the HetF protease. We further demonstrate that HetF and PatU3 have antagonistic actions in cell division and heterocyst differentiation. Based on all data available, we propose that HetF and PatU3 constitute a regulatory system for the coordination of cell division and heterocyst development in filamentous cyanobacteria.

Results

Identification of *patU3* by Suppressor Screening of a Δ*hetF* Mutant. To understand the functions of HetF in the regulation of cell division and heterocyst differentiation, we sought to determine the genetic pathway involving *hetF*. Since Δ*hetF* does not differentiate heterocyst and is thus unable to grow under diazotrophic conditions (27, 31, 32), we screened suppressors of Δ*hetF* on $BG11_0$ plates lacking combined nitrogen. 40 suppressor mutants were obtained under such conditions, indicating that they recovered the ability to develop functional heterocysts (Fig. 1). One of them, Δ*hetF*-s-1, was subjected to whole genome sequencing, and the results revealed a nonsense

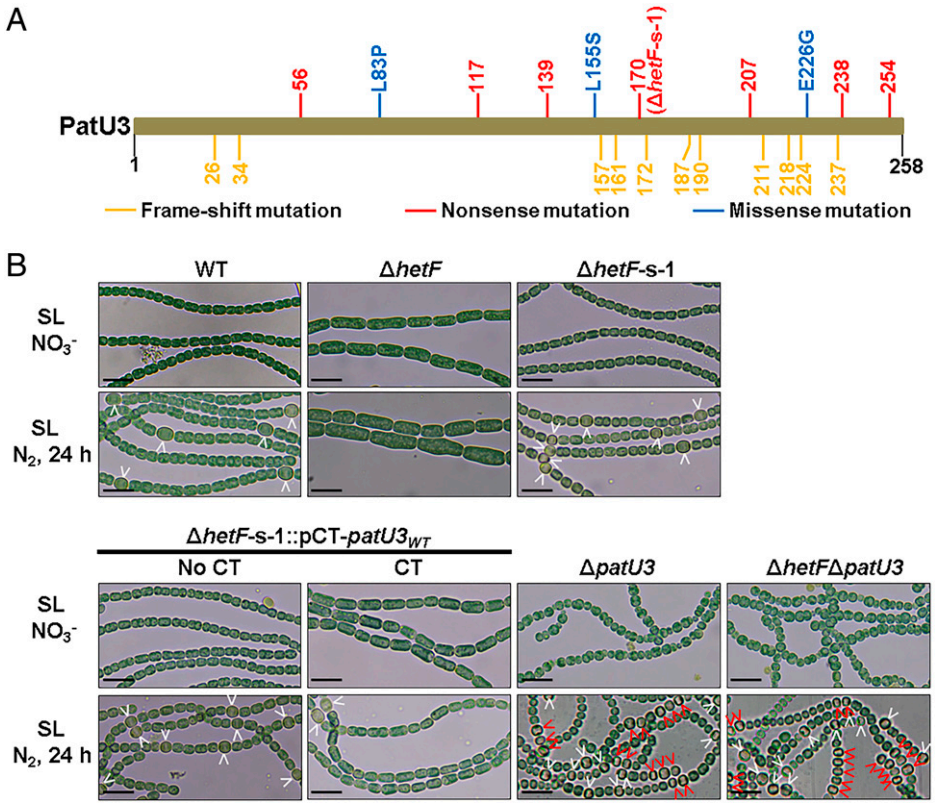

Fig. 1. *patU3* inactivation suppresses the phenotype of Δ*hetF*. (*A*) The schematic representation of frameshift, missense, and nonsense mutations in PatU3 sequence based on the analysis of 40 suppressors of Δ*hetF*. Δ*hetF*-s-1 was one of the suppressors of Δ*hetF*. (*B*) Suppressor mutation (Δ*hetF-s-1*) or deletion of *patU3* (Δ*hetF*Δ*patU3*) restored the ability of cell division and heterocyst differentiation in Δ*hetF*. For complementation of Δ*hetF*-s-1, a replicative plasmid bearing WT *patU3* under the control of inducible CT promoter was conjugated into Δ*hetF*-s-1, leading to Δ*hetF*-s-1::pCT-$patU3_{WT}$. Strains were cultured under SL with NO_3^- (BG11) or without NO_3^- ($BG11_0$, N_2). CT, 0.6 μM $CuSO_4$ and 4 mM theophylline for induction of *patU3* expression. White arrows indicate single heterocysts. Red arrows indicate Mch. (Scale bars, 10 μm).

mutation from a guanine base to an adenine at position 510 of the *patU3* coding region, leading to a truncated form of PatU3 with only the first 170 amino acid residues (Fig. 1*A*). Additional mutations were also identified in Δ*hetF*-s-1, but they were either in the intergenic regions or did not change the amino acid sequence of the corresponding proteins. Microscopic observation of the Δ*hetF*-s-1 mutant showed that the cells gained the ability to divide and differentiate heterocysts, consistent with its ability to grow under diazotrophic conditions (Fig. 1*B*). In contrast, Δ*hetF* displayed a cell-filamentation phenotype, and was unable to make heterocysts as previously reported (27). For the remaining 39 suppressor mutants, we amplified by PCR and sequenced the coding region of *patU3* together with a region covering 1,096 bp upstream of *patU3*. Strikingly, all of them contained mutations in the *patU3* coding region, corresponding to 21 mutation sites, including 11 frameshift mutations, and 10 missense or nonsense mutations (Fig. 1*A*).

To verify that inactivation of *patU3* suppressed the phenotypes of Δ*hetF*, we tried to express a full length *patU3* in the suppressor mutants. The phenotype of Δ*hetF* was highly unstable, as suppressor mutations frequently occurred during conjugation. Therefore, we performed inducer-dependent complementation of the suppressor mutant Δ*hetF*-s-1 with pCT-$patU3_{WT}$, a replicative plasmid carrying WT *patU3* under the control of the inducible CT promoter composed of the copper-inducible P_{petE} and the theophylline riboswitch (27, 34). In the absence of inducers for *patU3* expression, Δ*hetF*-s-1::pCT-$patU3_{WT}$ showed a phenotype similar to that of Δ*hetF*-s-1 with cell division and heterocyst formation (Fig. 1*B* and *SI Appendix*, Fig. S1A), although the heterocyst frequency was higher than that in the WT (*SI Appendix*, Fig. S1B). In contrast, induction of *patU3* expression caused cell filamentation and much less heterocysts, a phenotype similar to that of Δ*hetF* (Fig. 1*B* and *SI Appendix*, Fig. S1). The replicative plasmid was known to be present with varying copy numbers in different cells along the filament (35), which may account for the appearance of a few heterocysts.

To further confirm that *patU3* inactivation suppressed the effect of *hetF* deletion, we constructed a double mutant in which both *patU3* and *hetF* were inactivated (Δ*hetF*Δ*patU3*) by markerless, in-frame deletion (34). A single in-frame deletion of *patU3* (Δ*patU3*) was also obtained as a control. As previously reported (19), cultivation of Δ*patU3* with a combined nitrogen source led to production of cells with irregular and smaller size, and upon combined nitrogen deprivation, the formation of high frequency of heterocyst and Mch (Fig. 1*B* and *SI Appendix*, Fig. S1). The double mutant Δ*hetF*Δ*patU3* produced a similar phenotype as Δ*patU3*, completely abolishing the cell-division arrest and the lack of heterocyst formation observed in the Δ*hetF* single mutant. Note that Δ*hetF*Δ*patU3* showed a phenotype in cell size much stronger than that of the suppressor mutant Δ*hetF*-s-1 (Fig. 1*B*). This was likely due to the fact that the suppressor made a truncated, partially functional form of PatU3. These results altogether confirmed that the inactivation of *patU3* had a dominant effect on the inactivation of *hetF*, and indicated that *patU3* acted downstream of *hetF* in the same genetic pathway.

Ectopic Expression of *patU3* Mimics *hetF* Deletion and Blocks Cell Division by Inhibiting Septal PG Synthesis. Since inactivation of *patU3* allowed the Δ*hetF* mutant to divide and form heterocysts, we hypothesized that PatU3 might function as a negative regulator for cell division and heterocyst differentiation. To test this hypothesis, we checked if ectopic expression of *patU3* resulted in cell-division defect and cessation of heterocyst differentiation. Indeed, when *patU3* was overexpressed by the P_{rbcL} promoter on a replicative plasmid (pP_{rbcL}-*patU3*) in the WT background, cells showed a cell-division arrest phenotype similar to that of the Δ*hetF* mutant, and few heterocysts were formed after 24 h or 48 h of combined-nitrogen stepdown (Fig. 2 *A*–*C*). These results indicated that PatU3 was a division inhibitor and it functioned downstream of HetF to negatively control cell division and heterocyst differentiation.

To test if ectopic expression of *patU3* blocked cell division via a similar mechanism as *hetF* deletion, we checked the subcellular localization of FtsZ and septal PG synthesis. The replicative plasmid, pP_{rbcL}-*patU3*, was conjugated into a strain in which the WT allele of *ftsZ* was replaced by *ftsZ-cfp* fusion (27), leading to strain WT::*ftsZ-cfp*::pP_{rbcL}-*patU3*. As shown in Fig. 2 *D* and *E*, the Z-ring was still able to form in cells of WT::*ftsZ-cfp*::pP_{rbcL}-*patU3*, as one to three FtsZ-CFP ring-like structures, in proportion to cell length, were found in each elongated cell. This phenotype was similar to the localization of FtsZ in strain Δ*hetF*::*ftsZ-cfp* (27). Next, we checked the influence of *patU3* overexpression on septal PG remodeling using HADA (12). In the WT strain, cells divided normally and HADA fluorescence was observed at midcell and cell-cell junctions as expected (Fig. 2*F*). However, in the WT::pP_{rbcL}-*patU3* strain, no HADA labeling could be found in elongated cells, except at the cell-cell junctions that represented the cell poles from the precedent cell-division cycle (Fig. 2*F*). This labeling pattern was also similar to that of the Δ*hetF* strain, indicating that *patU3* overexpression blocked cell division by inhibiting septal PG synthesis but not FtsZ localization. Taken together, our results showed that ectopic expression of *patU3* produced a phenotype similar to that of *hetF* deletion by inhibiting cell division at the step of septal PG synthesis.

PatU3 Accumulates in the *hetF*-Deletion Mutant Under Conditions Leading to Inhibition of Cell Division or of Heterocyst Differentiation. The strikingly similar phenotypes following the ectopic expression of *patU3* and the deletion of *hetF* indicated that the accumulation of PatU3 might be responsible for the division arrest and lack of heterocyst formation in Δ*hetF*. To test if this was the case, we first compared PatU3 levels using Western blotting in WT and Δ*hetF* under different conditions using polyclonal antibodies raised against PatU3 (Fig. 3 *A* and *B*). As shown in Fig. 3*A*, PatU3 was below the detection level in WT under all conditions tested even with long exposure time (a band present in all samples including that prepared from Δ*patU3*, corresponded to a nonspecific protein recognized by the serum, as its molecular weight was much higher than that of PatU3). However, in the Δ*hetF* mutant, PatU3 was identified under several growth conditions where the absence of HetF induced a strong cell-filamentation phenotype or no heterocyst differentiation (27, Fig. 3*B*). The antibody was specific since the detected protein had a molecular weight similar to that of purified PatU3, and it was missing in the Δ*patU3* mutant. The nonspecific band present in Fig. 3*A* was no longer detected here, likely because a shorter exposure time was used, and the presence of relatively large amounts of PatU3 in several samples made the antibody less likely to react with a nonspecific target. PatU3 was detected in Δ*hetF* cells in the presence of nitrate as a combined nitrogen source, or weakly in the presence of ammonium, illuminated under standard light intensity. These conditions were known to induce a strong cell-division phenotype in the Δ*hetF* mutant (27, Fig. 3*B*), consistent with the inhibitory role of PatU3 in cell division. In contrast, no PatU3 accumulation was found under low-light illumination, conditions

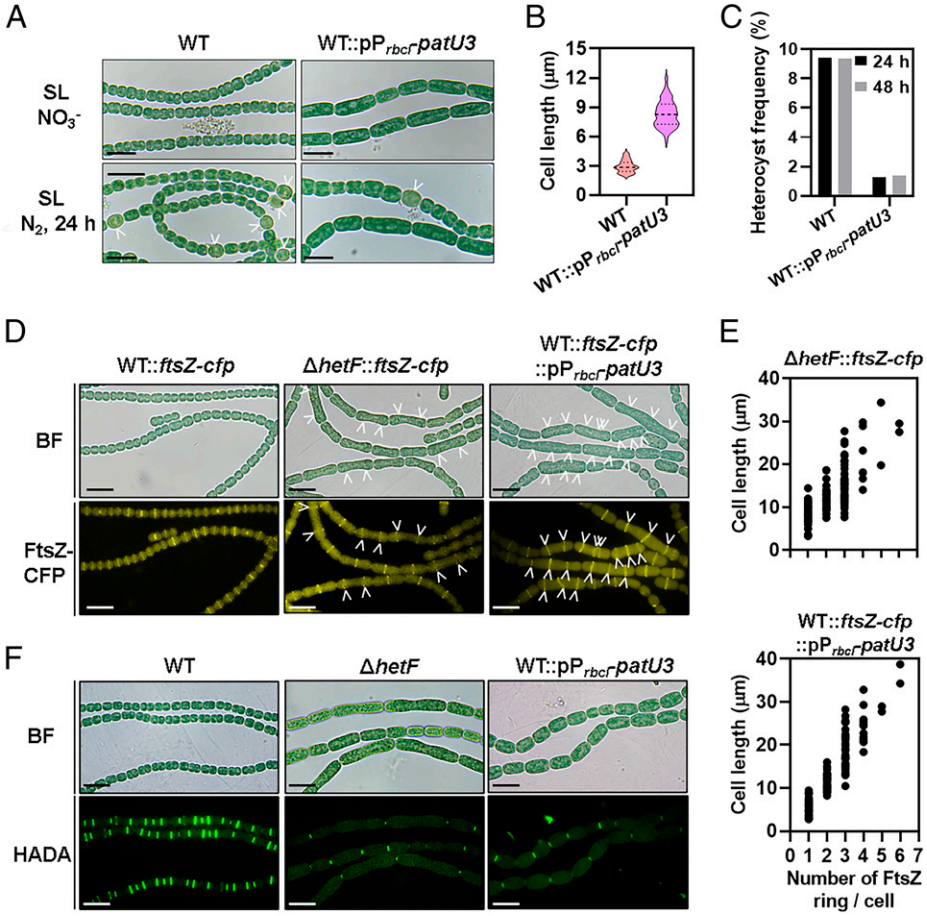

Fig. 2. *patU3* overexpression inhibits heterocyst differentiation and septal PG synthesis. (*A*) Microscopic observation of WT and WT::pP$_{rbcL}$-*patU3* cultured under SL in BG11 (NO_3^-) or $BG11_0$ (N_2) for 24 h. White arrows indicate heterocysts. (*B*) Cell length analysis of strains in *A*. Two hundred cells were measured for each sample. (*C*) Heterocyst frequency of strains in *A* after combined nitrogen deprivation for 24 h or 48 h. For each sample, 1,000 cells were used for the analysis. (*D*) FtsZ ring formation in WT::*ftsZ-cfp*, Δ*hetF*::*ftsZ-cfp*, and WT::*ftsZ-cfp*::pP$_{rbcL}$-*patU3* grown in BG11 under SL. White arrows indicate FtsZ-CFP rings in some elongated cells. (*E*) Relationship between the number of FtsZ ring per cell and cell length in Δ*hetF*::*ftsZ-cfp* and WT::*ftsZ-cfp*::pP$_{rbcL}$-*patU3*. 160 cells of Δ*hetF*::*ftsZ-cfp* and 209 cells of WT::*ftsZ-cfp*::pP$_{rbcL}$-*patU3* were analyzed, respectively. (*F*) Septal PG synthesis probed by HADA labeling of cells in BG11 under SL. (Scale bars in *A, D*, and *F*, 10 μm).

which repressed cell-division phenotype of the Δ*hetF* mutant (27, Fig. 3*B*). Thus, in the presence of a combined nitrogen source, whenever cell-division arrest took place for the Δ*hetF* mutant, PatU3 accumulation occurred. Under conditions inducing heterocyst differentiation (in the absence of a combined nitrogen source), PatU3 accumulated independently of light conditions (Fig. 3*B*), consistent with the inhibition of heterocyst differentiation in the mutant (27). Note that the same culture conditions necessary for PatU3 accumulation seen in Δ*hetF* led to a higher level of *hetF* expression in the WT (27). Thus, deletion of *hetF* led to accumulation of PatU3 in vivo.

HetF Degrades PatU3. The above results indicated that HetF controlled the level of PatU3 in *Anabaena*. HetF is a putative protease, related to the eukaryotic separase belonging to the family C50 of the Clan CD peptidases (32, 36). A mutation of the conserved Cys_{295} residue at the putative catalytic domain led to a loss-of-function phenotype for HetF (32), but neither its enzyme activity nor its substrate was known. Considering the genetic relationship between *patU3* and *hetF*, we checked if PatU3 could be a substrate for the HetF protease activity. To get soluble HetF, we expressed HetF without its transmembrane domain (TM) and the periplasmic tetratrico peptide repeats (TPRs) domain, but the conserved caspase HetF associated with TPRs (CHAT) domain with the putative catalytic site remained (Fig. 3*C*). The corresponding recombinant polypeptide was termed HetFCHAT. HetFCHAT produced under the control of an inducible promoter could restore the ability of cell division and heterocyst differentiation of Δ*hetF* (*SI Appendix*, Fig. S2A). We also tried various strategies to get soluble form of PatU3 in *Escherichia coli*, but only the fusion of a His-tagged GFP at the N terminus of PatU3 was soluble, named as GFP-PatU3 here. A GFP-PatU3 fusion was functional since its production could complement the phenotype of Δ*patU3* (*SI Appendix*, Fig. S2B).

As shown in Fig. 3*D*, when GFP-PatU3 was incubated with HetFCHAT, two smaller protein fragments appeared, with an apparent molecular weight of 43.7 kDa and 16.1 kDa, respectively. The amount of GFP-PatU3 decreased with time while that of the two digested products increased (Fig. 3 *D* and *E*). Both products were detected by using antibody against PatU3, but only the larger fragment (N-GFP-PatU3) reacted to an antibody against GFP (Fig. 3*D*), suggesting that the smaller protein fragment (C-GFP-PatU3) contained the C-terminal part of PatU3. As expected, GFP-PatU3 incubated alone or with $HetFCHAT_{C295A}$ remained intact (Fig. 3*D*), and no digestion of GFP was detected after incubation with HetFCHAT under the same assay conditions (*SI Appendix*, Fig. S3A). These results confirmed that HetF was a protease with PatU3 as a substrate.

It was reported that HetR accumulated to a high level when *hetF* was inactivated (28). We therefore tested whether HetF

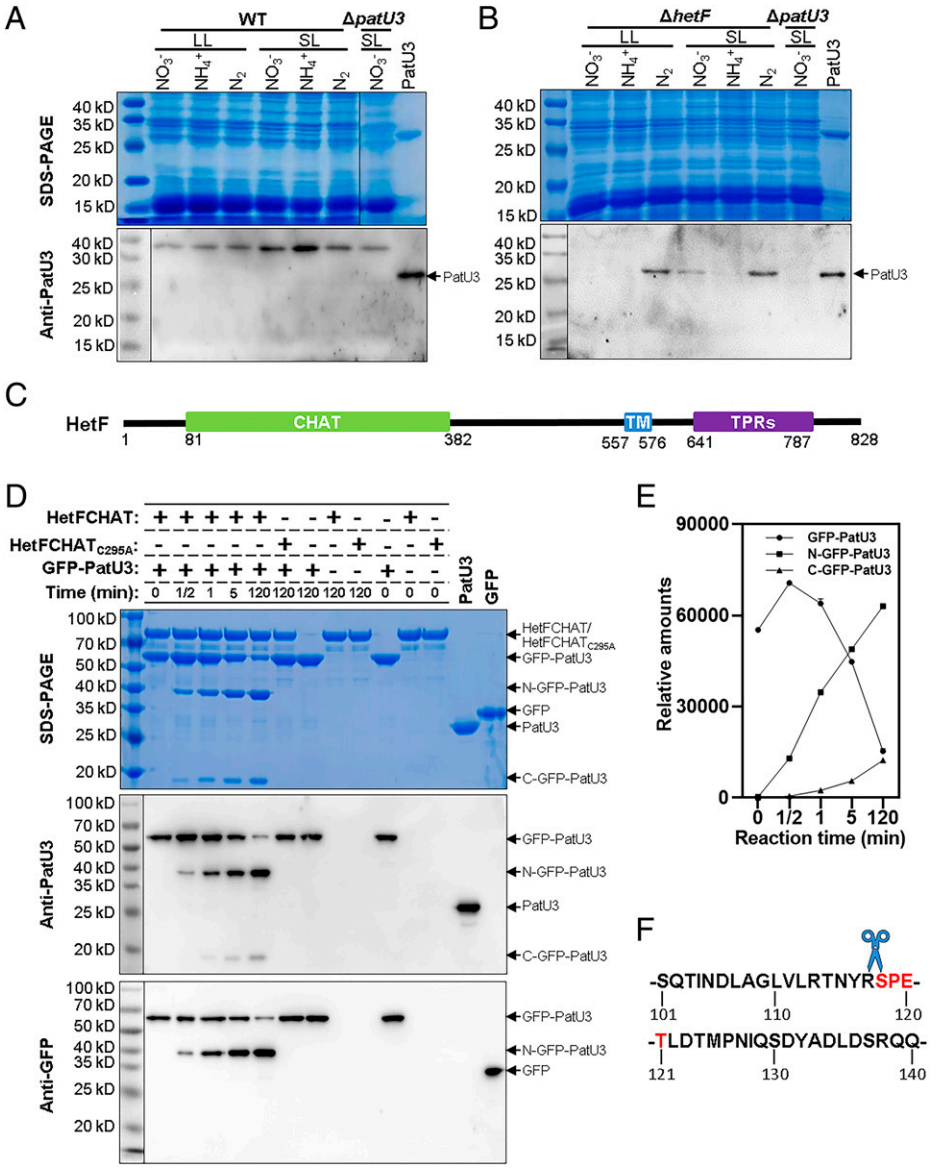

Fig. 3. PatU3 is a substrate of HetF. (*A* and *B*) Western blotting analysis of PatU3 levels in WT (*A*) and Δ*hetF* (*B*) under different conditions. The nature of the nitrogen source and light intensity (LL, low light; SL, standard light) were indicated on the top of each lane. Similar amounts of total proteins extracted from different strains were loaded on the gel and stained with Coomassie blue (*Top*), and probed with polyclonal antibody against PatU3 (*Bottom*). To optimize the signal of purified recombinant PatU3 control, 2.5 μg of PatU3 were loaded in the gel used for Coomassie blue staining, and 2.5 ng of PatU3 were loaded for Western blotting. All other samples were kept with similar amounts for the duplicated gels. Note that the Western blotting images in *A* and *B* were obtained with different exposure times of 10 s and 3 s, respectively. (*C*) Domain organization of HetF. (*D*) Digestion of recombinant fusion protein GFP-PatU3 by the CHAT domain of HetF (HetFCHAT). $HetFCHAT_{C295A}$, similar to HetFCHAT but bearing a mutation of the conserved Cys295 residue at the catalytic site. After the reaction, as described in the section *Materials and Methods*, proteins were separated by SDS-PAGE, stained with Coomassie blue (*Top*), or analyzed by Western blotting using antibodies against PatU3 (*Middle*), or against GFP (*Bottom*). N-GFP-PatU3, the N-terminal GFP-PatU3 fragment; C-GFP-PatU3, the C-terminal GFP-PatU3 fragment. (*E*) Quantification of PatU3, or PatU3 fragments after treatment by HetFCHAT based on the Western blotting (Anti-PatU3) in *D*. (*F*) Schematic diagram of PatU3 cleavage site (scissor) by HetF, between R117 and S118, determined by sequencing of C-GFP-PatU3. The four amino acid residues determined by N-terminal sequencing are marked in red. See *SI Appendix*, Fig. S4 for original data.

could also digest HetR. No cleavage of HetR by HetFCHAT was found (*SI Appendix*, Fig. S3B). HetFCHAT also failed to cleave PatA (*SI Appendix*, Fig. S3C), another regulator of heterocyst differentiation (37).

Determination of the Cleavage Site in PatU3 by HetF. By protein N-terminal sequencing of C-GFP-PatU3, the cleavage site was determined to be between residues R_{117} and S_{118} of PatU3 (Fig. 3*F* and *SI Appendix*, Fig. S4). To further confirm this cleavage site, different mutations were introduced into PatU3 at R_{117}, as well as at several residues surrounding it. As shown in Fig. 4*A*, HetFCHAT cut PatU3 and its variants carrying single point mutation of T114A, N115A, Y116A, P119A, E120A, or T121A with similar efficiency. However, substitution of R117 by Ala, Asp, or His residues (R117A, R117D, and R117H) completely abolished the cleavage of PatU3 by HetFCHAT, consistent with the finding that HetF cleaved PatU3 at residue R117. PatU3 with the S118A mutation was also cleaved by HetFCHAT, with a decreased efficiency, likely because S118 lies immediately after R117, and thus may affect substrate recognition.

To confirm that the cleavage of PatU3 by HetF was critical for its regulation, we tested the effect of the above mutations in PatU3 in vivo by ectopic production of PatU3 or its variants. As already shown in Fig. 2, when *patU3* was expressed in the WT background under the control of P_{rbcL}, one of the strongest promoters in cyanobacteria, it could inhibit cell division

and heterocyst differentiation. However, when the CT promoter was used to drive the expression of *patU3* (pCT-$patU3_{WT}$), no particular effect was observed after induction (Fig. 4*B*). Accordingly, Western blotting detected strong accumulation of PatU3 expressed with P_{rbcL}, but not with the CT promoter (*SI Appendix*, Fig. S5). These results, together with the fact that PatU3 was undetectable by Western blotting under the assay conditions in the WT (Figs. 3*A* and 4*C* and *SI Appendix*, Fig. S5), suggested that PatU3 was under strong proteolytic pressure exerted by HetF. However, when $patU3_{R117A}$, $patU3_{R117D}$, or $patU3_{R117H}$ was expressed by the CT promoter, cell division was arrested, and heterocyst frequency dramatically decreased; concomitantly, these PatU3 variants accumulated in the cells. These results confirmed the cleavage site of PatU3 at R117 by HetF in vivo (Fig. 4 *B* and *C* and *SI Appendix*, Figs. S6 and S7). Other mutations in PatU3 that did not prevent proteolysis by HetF failed to accumulate in the cells, and to cause a particular phenotype (Fig. 4 *B* and *C* and *SI Appendix*, Figs. S6 and S7). These results indicated that the cleavage of PatU3 at R117 by HetF is critical for PatU3 regulation in vivo.

Discussion

HetF has long been predicted as a protease (32, 36), but neither its activity nor its substrate has been reported. We showed here that PatU3 was cleaved by HetF into two fragments after the residue R117. This cleavage property was commonly found for the family C50 of the Clan CD peptidases, with a preference for Arg residue at the cleaving site (MEROPS peptidase database, merops.sanger.ac.uk, 36, 38). The processed protein products were then further degraded by the general proteolytic pathway in the cells.

The inactivation of *hetF* led to two phenotypes: cell-division arrest and lack of heterocyst differentiation (27). It is known that inhibition of cell division is accompanied by a failure of heterocyst differentiation (26). Therefore, the two events could be controlled by a common mechanism. Our data reported here indicated that this control mechanism was accomplished by the level of PatU3 under check by the protease HetF. The accumulation of PatU3 found in the *hetF* deletion mutant, the effect of PatU3 ectopic expression or the expression of PatU3 variants altering the R117 residue, all indicated that HetF exerted its functions by controlling the levels of PatU3 in the cells. How then does this proteolytic pathway regulate the two processes? Based on our study and the interaction previously reported between PatU3 and HetZ or PatU3 and Ftn6 (20, 25), we propose a model for the action of HetF and PatU3 in the regulation of cell division and heterocyst differentiation (Fig. 5). In the WT, PatU3 is cleaved by HetF at the division site, and is thus unable to inhibit cell division through interaction with Ftn6.

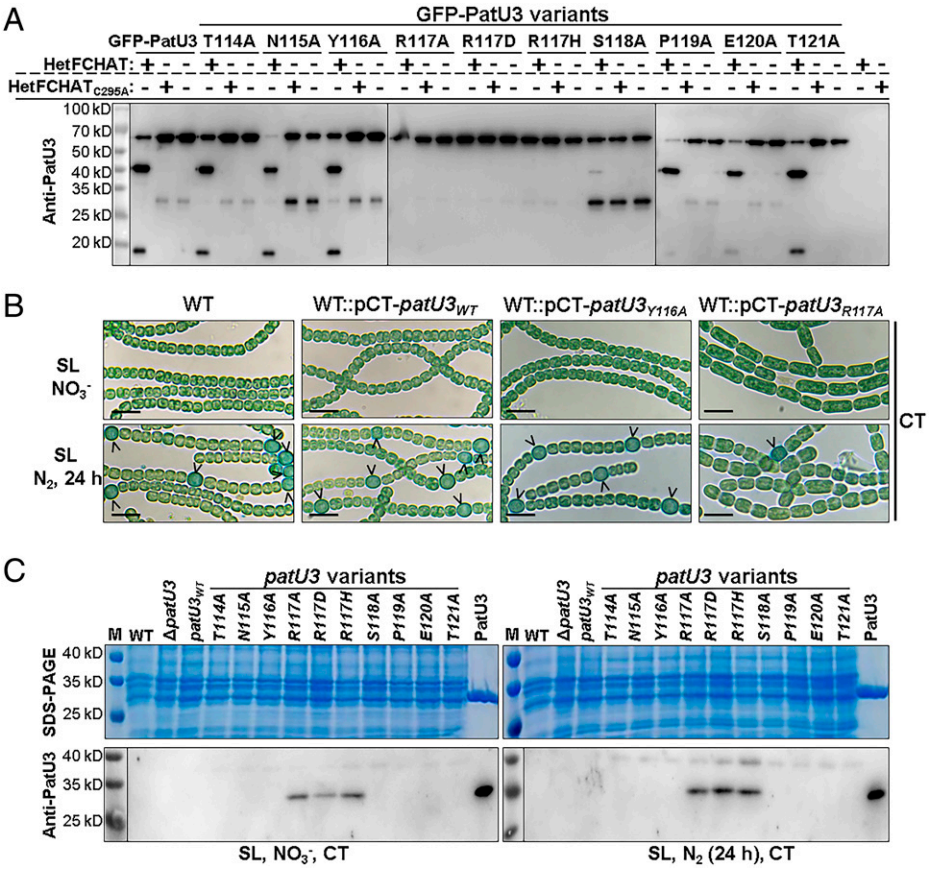

Fig. 4. Mutation of the cleavage site of PatU3 by HetF leads to cell-division defect, dramatically decreased heterocyst frequency, and PatU3 accumulation. (*A*) WT GFP-PatU3, or its variants with mutation at the residue R117 at the cleavage site by HetF, or mutation at residues around R117 (from T114 to T121), were incubated individually with HetFCHAT. Samples were analyzed by Western blotting using antibody against PatU3. (*B*) Effect of PatU3 mutations on cell division and heterocyst differentiation. Plasmids expressing different versions of *patU3* (see *A*) under the control of pCT, were conjugated into the WT. $CuSO_4$ at 0.6 μM and theophylline at 4 mM (CT) were used to induce *patU3* expression for 72 h. All images of the strains were taken after cultivation in BG11 (NO_3^-) or $BG11_0$ (N_2) for 24 h under SL. Arrows indicate heterocysts, which were stained by Alcian blue. (Scale bars, 10 μm). (*C*) Western blotting analysis of the production levels of PatU3 or its variants in strains cultivated with CT inducers shown in *B* and *SI Appendix*, Fig. S6, using polyclonal antibody against PatU3. To optimize the signal of purified recombinant PatU3 control, 10 μg of PatU3 were loaded in the gel used for Coomassie blue staining, and 10 ng of PatU3 were loaded for Western blotting. All other samples were kept with similar amounts for the duplicated gels.

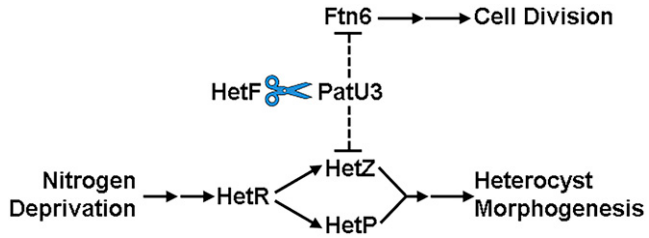

Fig. 5. A model on the action of the HetF-PatU3 proteolytic pathway in the regulation of cell division and heterocyst differentiation. PatU3 inhibits cell division and heterocyst differentiation through interaction with Ftn6 and HetZ, respectively, although the mechanism of PatU3 inhibition remains to be understood (dashed lines). The amount of PatU3 is limited by proteolysis by HetF (indicated by a scissor) in order for cell division and heterocyst differentiation to proceed. In the absence of HetF, PatU3 accumulates to block cell division. Meanwhile, heterocyst differentiation is initiated by HetR, but failed to move to the morphogenesis step because of the sequestration of HetZ by PatU3. HetP, together with HetZ, is necessary for developmental commitment, a step between initiation and morphogenesis in the process of heterocyst differentiation. See *Discussion* for additional regulators, such as PatA and PatN, potentially involved in the coordination of cell division and heterocyst differentiation.

The amount of PatU3 is thus limited through the action of HetF to a low level, as low as undetectable by our Western blotting, yet sufficient to sequester part of HetZ, to limit heterocyst differentiation to a standard level observed in the WT (without Mch). In the Δ*hetF* mutant, PatU3 accumulates; the high amount of PatU3 interacts with Ftn6 to inhibit cell division on the one hand and sequesters HetZ to inhibit heterocyst differentiation on the other. In the Δ*patU3* mutant or the Δ*hetF*Δ*patU3* double mutant, the inhibitory effect of PatU3 on cell division is completely missing, leading to cells of smaller and irregular size; at the same time, all HetZ is freely available, mimicking HetZ overproduction, thus leading to Mch (24). Certain details of the model will still need to be worked out in the future, in particular on the inhibitory mechanisms of PatU3 on Ftn6 and HetZ. Nevertheless, this model can adequately explain the accumulation of HetR observed in the *hetF*-deficient mutant, which did not cause Mch (31, 32). The increase in HetR level indicates that the initiation of heterocyst differentiation is accomplished in the absence of *hetF*. However, since HetZ, together with HetP, is necessary for the commitment step (2, 7–11, Fig. 5), morphogenesis cannot take place when HetZ is sequestered by PatU3 in the Δ*hetF* mutant. Therefore, we propose that HetF regulates the commitment step, instead of the early step of heterocyst differentiation as proposed previously (31–33).

In addition to the regulators proposed in the model as shown in Fig. 5, several other proteins, such as PatN and PatA, may also play a role in the coordination of cell division and heterocyst differentiation (17, 20, 39–42). In *Nostoc punctiforme*, PatN has been shown to be a negative regulator of heterocyst differentiation, and displays a biased inheritance in two daughter vegetative cells (39). Such a distribution pattern of PatN was proposed to act as a mechanism allowing one of the two daughter cells to initiate heterocyst differentiation (39). A cell-division arrest may interfere with cellular distribution of PatN, and thus repress heterocyst differentiation. PatN may regulate the level of PatA and HetZ, and was shown to interact with PatU3, although the implication of PatU3-PatN interaction is unknown (17, 39).

Our studies revealed a distinct proteolytic pathway for the coordination between cell division and heterocyst differentiation. This coordination may provide a control on the timing of heterocyst differentiation relative to the cell cycle. The newborn cell before the divisome is fully assembled may be prevented from becoming a heterocyst by a transient accumulation of PatU3, which may explain why heterocyst is bigger in cell size than vegetative cell in general. The results reported here paved the way for further studies on the intimate link between cell division and heterocyst differentiation, a unique model for prokaryotic developmental biology.

Materials and Methods

Strains and Growth Conditions. The procedures for the construction of *Anabaena* mutants are described in detail in the *SI Appendix*. All plasmids and primers used for strain construction and genotype verification were listed in *SI Appendix*, Tables S1 and S2, respectively. All strains used in this study were listed in *SI Appendix*, Table S3. *Anabaena* strains were cultivated in BG11 (43) or $BG11_0$ ($BG11_0$ without nitrate) media, with shaking (30 °C, 180 rpm) and standard light illumination of 30 μmol photons $m^{-2}s^{-1}$ (SL). When necessary, cultures were incubated at low light illumination of 7 μmol photons $m^{-2}s^{-1}$ (LL). The strains that have cell-division arrest phenotype, like Δ*hetF*, were precultured and stocked in $BG11_0$ with 2.5 mM NH_4Cl and LL. The phenotype of cell-division defect could be induced by cultivating in BG11 under SL with an initial OD_{750} of 0.08 to 0.3 for 2 to 4 d. When needed, 100 μg mL^{-1} neomycin or 5 μg mL^{-1} spectinomycin and 2.5 μg mL^{-1} streptomycin, were added to the cultures.

Polyclonal Antibody Production and Western Blotting. The plasmid pET28-PatU3 was constructed by inserting the *patU3* coding sequence (1 to 774 bp, amplified with primers Palr0101F1c/Palr0101R774a) into pET28a. The fusion protein contains PatU3 and a 6His-tag at its N terminus. To induce protein expression, *E. coli* BL21 (DE3) cells containing pET28-PatU3 were grown in Luria-Bertani (LB) medium with 0.5 mM β-D-1-thiogalactopyranoside (IPTG) at 37 °C. After induction for 4 h, cells were collected by centrifugation, resuspended in a lysis buffer (pH 7.4, 137 mM NaCl, 2.7 mM KCl, 8 mM Na_2HPO_4, 14.6 mM KH_2PO_4), and lysed by JN minilow temperature and ultrahigh pressure cell breaker (JNBIO Co. Ltd.). The lysate was centrifuged at 10,000 rpm for 40 min at 4 °C. The precipitate (inclusion body) was washed twice with 2 M urea, and used for polyclonal antibody production by Frdbio Co. Ltd.

With a starting OD_{750} of 0.08, WT and Δ*hetF* were cultivated for 2 d, respectively, under different light intensities and nitrogen regimes. Samples were collected by filtration and broken with FastPrep-24 (6.0 m/s, 60 s) in LDS loading buffer [70 mM lithium dodecyl sulfate, 100 mM Tris·HCl, pH 8.5, 10% glycerol, 4 mM ethylenediaminetetraacetic acid (EDTA), 0.025% Coomassie brilliant blue G250]. Cell extracts were boiled at 95 °C for 10 min, followed by centrifugation at 135,000 rpm for 10 min. The supernatant was subjected to immunoblot assay with a polyclonal antibody against PatU3.

Protein Production and Purification. All protein expression plasmids used in this study and related primers were listed in *SI Appendix*, Tables S1 and S2. All the recombinant proteins were purified with a routine procedure. Briefly, Rosetta 2 (DE3) containing the protein expression plasmid was grown in LB medium at 37 °C. When the culture reached the density of $OD_{600} = 0.5$, 0.5 mM IPTG was added. After 16 h of induction at 16 °C, cells were harvested by centrifugation, resuspended in lysis buffer (1 M NaCl, 20 mM Tris·HCl, pH 8.0), and broken by JN minilow temperature and ultrahigh pressure cell breaker (JNBIO Co. Ltd.). The lysate was centrifuged at 10,000 rpm for 40 min at 4 °C, and the recombinant protein in the lysate was purified using a Ni-NTA affinity column (Qiagen) according to the product manual. The protein eluted from the Ni-NTA column was further purified using a 120 mL gel filtration column (ÄKTA avant). The purified proteins (in the buffer of 20 mM Tris·HCl, 150 mM NaCl, 5% glycerol, pH8.0) were preserved at −80 °C. Protein purity was estimated by sodium dodecyl sulfate-polyacrylamide gel electrophoresis (SDS-PAGE), and protein concentration was quantified by Bradford assay using bovine serum albumin (BSA) as standard.

Enzymatic Activity Assay of HetF. To test the cystine peptidase activity of HetF, HetFCHAT (50 μg) and a potential substrate (50 μg) were incubated at 37 °C in a 100-μL mixture containing 20 mM Tris·HCl (pH 8.0) and 150 mM

NaCl. Ten- to 20-μL samples taken at different time points were analyzed by SDS-PAGE. To estimate the place of cleave within GFP-PatU3 by Western blot, all the samples of cleavage reaction were diluted one hundred times, separated by 10% SDS-PAGE, and then subjected to Western blot assay using polyclonal antibody against PatU3 or monoclonal antibody against GFP.

Microscopy. A SDPTOP EX30 microscope was used to take brightfield images, and an EPI fluorescence microscope SDPTOP EX40 to take fluorescent images. The filter (EX379-401, DM420LP, EM435-485) was used to picture HADA fluorescence (exposure time: 200 ms). The filter (EX426-446, DM455LP, EM460-500) was used for CFP fluorescence images (exposure time: 1 s). All images were processed using ImageJ without deconvolution.

Data, Materials, and Software Availability. All study data are included in the article and/or supporting information.

ACKNOWLEDGMENTS. This work was supported by the National Natural Science Foundation of China (Grant No. 92051106), the Key Research Program of Frontier Sciences of the Chinese Academy of Sciences (Grant No. QYZDJ-SSW-SMC016), the Featured Institute Service Projects from the Institute of Hydrobiology, the Chinese Academy of Sciences (Grant No. Y85Z061601), the Hubei Province Postdoctoral Innovation Research Post Project, the Special Research Assistant Project CAS, and the Excellent Youth Program of "Wuhan Talent." We thank Shishen Du, Professor at the Wuhan University, for critical comments of the manuscript, and an anonymous reviewer for insightful comments that helped us to improve the discussion section.

1. Y. Budirahardja, P. Gönczy, Coupling the cell cycle to development. *Development* **136**, 2861–2872 (2009).
2. X. Zeng, C.-C. Zhang, The making of a heterocyst in cyanobacteria. *Annu. Rev. Microbiol* 10.1146/annurev-micro-041320-093442 (2022).
3. A. Herrero, J. Stavans, E. Flores, The multicellular nature of filamentous heterocyst-forming cyanobacteria. *FEMS Microbiol. Rev.* **40**, 831–854 (2016).
4. C. P. Wolk, A. Ernst, J. Elhai, "Heterocyst metabolism and development" in *The Molecular Biology of Cyanobacteria*, D. A. Bryant, Ed. (Springer Netherlands, 1994), pp. 769–823.
5. W. J. Buikema, R. Haselkorn, Characterization of a gene controlling heterocyst differentiation in the cyanobacterium *Anabaena* 7120. *Genes Dev.* **5**, 321–330 (1991).
6. W. J. Buikema, R. Haselkorn, Expression of the *Anabaena hetR* gene from a copper-regulated promoter leads to heterocyst differentiation under repressing conditions. *Proc. Natl. Acad. Sci. U.S.A.* **98**, 2729–2734 (2001).
7. Y. Du, Y. Cai, S. Hou, X. Xu, Identification of the HetR recognition sequence upstream of *hetZ* in *Anabaena* sp. strain PCC 7120. *J. Bacteriol.* **194**, 2297–2306 (2012).
8. B. L. Flaherty, D. B. F. Johnson, J. W. Golden, Deep sequencing of HetR-bound DNA reveals novel HetR targets in *Anabaena* sp. strain PCC7120. *BMC Microbiol.* **14**, 255 (2014).
9. P. Videau *et al.*, The heterocyst regulatory protein HetP and its homologs modulate heterocyst commitment in *Anabaena* sp. strain PCC 7120. *Proc. Natl. Acad. Sci. U.S.A.* **113**, E6984–E6992 (2016).
10. H. Zhang, S. Wang, Y. Wang, X. Xu, Functional overlap of *hetP* and *hetZ* in regulation of heterocyst differentiation in *Anabaena* sp. strain PCC 7120. *J. Bacteriol.* **200**, e00707-17 (2018).
11. H. Zhang, X. Xu, Manipulation of pattern of cell differentiation in a *hetR* mutant of *Anabaena* sp. PCC 7120 by overexpressing *hetZ* alone or with *hetP*. *Life (Basel)* **8**, 60 (2018).
12. J.-Y. Zhang, G.-M. Lin, W.-Y. Xing, C.-C. Zhang, Diversity of growth patterns probed in live cyanobacterial cells using a fluorescent analog of a peptidoglycan precursor. *Front. Microbiol.* **9**, 791 (2018).
13. H. S. Yoon, J. W. Golden, Heterocyst pattern formation controlled by a diffusible peptide. *Science* **282**, 935–938 (1998).
14. J. Elhai, I. Khudyakov, Ancient association of cyanobacterial multicellularity with the regulator HetR and an RGSGR pentapeptide-containing protein (PatX). *Mol. Microbiol.* **110**, 931–954 (2018).
15. I. Khudyakov, G. Gladkov, J. Elhai, Inactivation of three RG(S/T)GR pentapeptide-containing negative regulators of HetR results in lethal differentiation of *Anabaena* PCC 7120. *Life (Basel)* **10**, 326 (2020).
16. S. M. Callahan, W. J. Buikema, The role of HetN in maintenance of the heterocyst pattern in *Anabaena* sp. PCC 7120. *Mol. Microbiol.* **40**, 941–950 (2001).
17. D. D. Risser, S. M. Callahan, Genetic and cytological evidence that heterocyst patterning is regulated by inhibitor gradients that promote activator decay. *Proc. Natl. Acad. Sci. U.S.A.* **106**, 19884–19888 (2009).
18. L. Corrales-Guerrero, V. Mariscal, E. Flores, A. Herrero, Functional dissection and evidence for intercellular transfer of the heterocyst-differentiation PatS morphogen. *Mol. Microbiol.* **88**, 1093–1105 (2013).
19. W. Zhang *et al.*, A gene cluster that regulates both heterocyst differentiation and pattern formation in *Anabaena* sp. strain PCC 7120. *Mol. Microbiol.* **66**, 1429–1443 (2007).
20. C. Li, H. Zhang, Y. Du, W. Zhang, X. Xu, Effects of PatU3 peptides on cell size and heterocyst frequency of *Anabaena* sp. strain PCC 7120. *J. Bacteriol.* **203**, e0010821 (2021).
21. S. Y. Miyagishima, C. P. Wolk, K. W. Osteryoung, Identification of cyanobacterial cell division genes by comparative and mutational analyses. *Mol. Microbiol.* **56**, 126–143 (2005).
22. M. Marbouty, C. Saguez, C. Cassier-Chauvat, F. Chauvat, Characterization of the FtsZ-interacting septal proteins SepF and Ftn6 in the spherical-celled cyanobacterium *Synechocystis* strain PCC 6803. *J. Bacteriol.* **191**, 6178–6185 (2009).
23. O. A. Gorelova, O. I. Baulina, U. Rasmussen, O. A. Koksharova, The pleiotropic effects of *ftn2* and *ftn6* mutations in cyanobacterium *Synechococcus* sp. PCC 7942: An ultrastructural study. *Protoplasma* **250**, 931–942 (2013).
24. P. Videau *et al.*, The *hetZ* gene indirectly regulates heterocyst development at the level of pattern formation in *Anabaena* sp. strain PCC 7120. *Mol. Microbiol.* **109**, 91–104 (2018).
25. Y. Du *et al.*, Expression from DIF1-motif promoters of *hetR* and *patS* is dependent on HetZ and modulated by PatU3 during heterocyst differentiation. *PLoS One* **15**, e0232383 (2020).
26. S. Sakr, R. Jeanjean, C.-C. Zhang, T. Arcondeguy, Inhibition of cell division suppresses heterocyst development in *Anabaena* sp. strain PCC 7120. *J. Bacteriol.* **188**, 1396–1404 (2006).
27. W.-Y. Xing *et al.*, HetF protein is a new divisome component in a filamentous and developmental cyanobacterium. *MBio* **12**, e0138221 (2021).
28. X. Yang *et al.*, GTPase activity-coupled treadmilling of the bacterial tubulin FtsZ organizes septal cell wall synthesis. *Science* **355**, 744–747 (2017).
29. A. J. F. Egan, J. Errington, W. Vollmer, Regulation of peptidoglycan synthesis and remodelling. *Nat. Rev. Microbiol.* **18**, 446–460 (2020).
30. L. Wang *et al.*, The developmental regulator PatD modulates assembly of the cell-division protein FtsZ in the cyanobacterium *Anabaena* sp. PCC 7120. *Environ. Microbiol.* **23**, 4823–4837 (2021).
31. F. C. Y. Wong, J. C. Meeks, The *hetF* gene product is essential to heterocyst differentiation and affects HetR function in the cyanobacterium *Nostoc punctiforme*. *J. Bacteriol.* **183**, 2654–2661 (2001).
32. D. D. Risser, S. M. Callahan, HetF and PatA control levels of HetR in *Anabaena* sp. strain PCC 7120. *J. Bacteriol.* **190**, 7645–7654 (2008).
33. A. M. Muro-Pastor, W. R. Hess, Heterocyst differentiation: From single mutants to global approaches. *Trends Microbiol.* **20**, 548–557 (2012).
34. T.-C. Niu *et al.*, Expanding the potential of CRISPR-Cpf1 based genome editing technology in the cyanobacterium *Anabaena* PCC 7120. *ACS Synth. Biol.* **8**, 170–180 (2019).
35. Y. Yang *et al.*, Phenotypic variation caused by variation in the relative copy number of pDU1-based plasmids expressing the GAF domain of Pkn41 or Pkn42 in *Anabaena* sp. PCC 7120. *Res. Microbiol.* **164**, 127–135 (2013).
36. L. Aravind, E. V. Koonin, Classification of the caspase-hemoglobinase fold: Detection of new families and implications for the origin of the eukaryotic separins. *Proteins* **46**, 355–367 (2002).
37. J. Liang, L. Scappino, R. Haselkorn, The *patA* gene product, which contains a region similar to CheY of *Escherichia coli*, controls heterocyst pattern formation in the cyanobacterium *Anabaena 7120*. *Proc. Natl. Acad. Sci. U.S.A.* **89**, 5655–5659 (1992).
38. A. J. Barrett, N. D. Rawlings, Evolutionary lines of cysteine peptidases. *Biol. Chem.* **382**, 727–733 (2001).
39. D. D. Risser, F. C. Y. Wong, J. C. Meeks, Biased inheritance of the protein PatN frees vegetative cells to initiate patterned heterocyst differentiation. *Proc. Natl. Acad. Sci. U.S.A.* **109**, 15342–15347 (2012).
40. H. Masukawa, H. Sakurai, R. P. Hausinger, K. Inoue, Increased heterocyst frequency by patN disruption in *Anabaena* leads to enhanced photobiological hydrogen production at high light intensity and high cell density. *Appl. Microbiol. Biotechnol.* **101**, 2177–2188 (2017).
41. S. S. Young-Robbins, D. D. Risser, J. R. Moran, R. Haselkorn, S. M. Callahan, Transcriptional regulation of the heterocyst patterning gene *patA* from *Anabaena* sp. strain PCC 7120. *J. Bacteriol.* **192**, 4732–4740 (2010).
42. A. Valladares, C. Velázquez-Suárez, A. Herrero, Interactions of PatA with the divisome during heterocyst differentiation in *Anabaena*. *MSphere* **5**, e00188-20 (2020).
43. R. Rippka, J. Deruelles, J. B. Waterbury, M. Herdman, R. Y. Stanier, Generic assignment, strain histories and properties of pure cultures of cyanobacteria. *J. Gen. Microbiol.* **111**, 1–61 (1979).